Neogene basins in Eastern Rif of Morocco and their potential to host native sulphur

Laila Boubkari, Mohammed Achalhi, Otmane Raji, Muhammad Ouabid, Jean-Louis Bodinier, Imad El Kati, Hicham El Messbahi

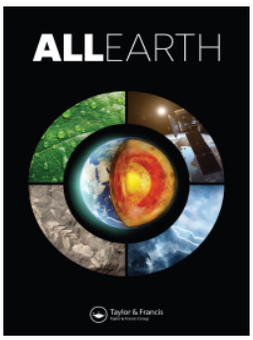

All Earth

ISSN: (Print) (Online) Journal homepage: https://www.tandfonline.com/loi/tgda21

Neogene basins in Eastern Rif of Morocco and their potential to host native sulphur

Laila Boubkari, Mohammed Achalhi, Otmane Raji, Muhammad Ouabid, Jean-Louis Bodinier, Imad El Kati & Hicham El Messbahi

To cite this article: Laila Boubkari, Mohammed Achalhi, Otmane Raji, Muhammad Ouabid, Jean-Louis Bodinier, Imad El Kati & Hicham El Messbahi (2022) Neogene basins in Eastern Rif of Morocco and their potential to host native sulphur, All Earth, 34:1, 90-106, DOI: 10.1080/27669645.2022.2097040

To link to this article: https://doi.org/10.1080/27669645.2022.2097040

Published online: 18 Jul 2022.

ALL EARTH
2022, VOL. 34, NO. 1, 90–106
https://doi.org/10.1080/27669645.2022.2097040

Taylor & Francis
Taylor & Francis Group

LITHOSPHERE

OPEN ACCESS Check for updates

Neogene basins in Eastern Rif of Morocco and their potential to host native sulphur

Laila Boubkari[a], Mohammed Achalhi[b], Otmane Raji[a], Muhammad Ouabid[a], Jean-Louis Bodinier[a,c], Imad El Kati[d] and Hicham El Messbahi[d]

[a]Geology and Sustainable Mining, Mohammed VI Polytechnic University, Benguerir, Morocco; [b]Département des Sciences de la Terre, Ecole Nationale Supérieure Des Mines, Rabat, Morocco; [c]Geoscience Montpellier, University of Montpellier & CNRS, Montpellier, France; [d]Department of Geology, Sidi Mohamed Ben Abdallah University, Taza, Morocco

ABSTRACT

Sediment-hosted sulphur deposits provide valuable information on sedimentary biogeochemical processes related to microbial activity and are paleoenvironmental proxy records. They are also used as markers for oil exploration and the largest ones may represent exploitable economic resources of sulphur. Biogenic sulphur occurrences associated with Neogene formations are found around the Western Mediterranean, in Southern Europe (e.g. Hellin, Lorca, and Teruel, Spain, and Sicily, Italy). In northern Morocco, similar geological settings are present where several sediment-hosted sulphur occurrences were reported by unpublished studies. In this study, we provide the first description of such occurrences selected from two Neogene basins in the Eastern Rif (Taza-Guercif and Boudinar) and studied using sedimentological facies analysis and mineralogical data. The studied facies occur as yellowish sub-spherical concretions, nodules, and laminated structures associated with gypsiferous marls or organic-matter-rich marly clays and gypsum lenses. Mineralogical analysis revealed a mineralogical assemblage composed mainly jarosite, gypsum, and native sulphur. These geo-markers are indicative of bacterially mediated sulphate reduction and favourable conditions for the formation of sulphur, especially at the level of the Guercif basin. In contrast, Ras Tarf volcanism probably contributed to the observed facies in the Boudinar basin through different processes.

ARTICLE HISTORY
Received 2 February 2022
Accepted 29 June 2022

KEYWORDS
Native sulphur; Neogene; Rif; Morocco

1. Introduction

Elemental sulphur (S) is essential for many industrial applications ranging from fertilisers, sulphuric acid, and construction industry to emerging uses such as polymer industry, batteries, and thermal energy storage (Kutney, 2007; Wagenfeld et al., 2019). It is widely distributed on the Earth but rarely found in native form. Notable exceptions include sulphur deposits associated with volcanic hydrothermal systems, primarily along the Pacific Ring of Fire whose deposits are mined in Indonesia (e.g. Newhall & Dzurisin, 1988; Scher et al., 2013). In this setting, native sulphur is commonly associated with iron oxides and sulphur-bearing minerals including gypsum, pyrite, jarosite and natrojarosite, produced by hydrothermal alteration and sublimate fumarolic deposits (Rodríguez & van Bergen, 2017; Serafimovski et al., 2015). A second type of native sulphur deposit leading to significant accumulations is associated with salt diapirs as part of caprock assemblages or with sulphate-rich lithologies as stratabound mineralisation (Labrado et al., 2019; Ruckmick et al., 1979). For the second type, biological processes are considered to play a pivotal role in the genesis and accumulations of native sulphur (Labrado et al., 2019; Machel, 2001).

Until recently, there was a consensus to ascribe native sulphur associated with evaporites to hydrocarbons coming into contact with sulphate minerals in a system supplied with O_2 resulting in oxidation of sulphides produced by sulphate-reducing bacteria (BSR). However, this model raises important difficulties regarding the formation of large sulphur deposits, as an excess of oxygen would negatively affect the microbial sulphate-reduction activity and sulphide-to-native sulphur conversion. Conditions difficult to achieve in nature would be needed, such as enormous oxygenised water quantities in an environment constantly supplied with hydrocarbon (Labrado et al., 2019). Thus, a new hypothesis has been proposed postulating the formation of native sulphur deposits by microbial activity without molecular oxygen supply (Labrado et al., 2019). This gives more consideration to the sulphate-reducing organisms through their capacity of shifting from harmful sulphide production to native sulphur production as less energy-yielding catabolism (Labrado et al., 2019). On the other hand, sulphates could also be reduced to sulphide abiotically through thermochemical sulphate reduction processes (TSR) during the late diagenetic and thermal events linked with metamorphic process (Barré

CONTACT Mohammed Achalhi achalhi@enim.ac.ma Département des Sciences de la Terre, Ecole Nationale Supérieure Des Mines, Rabat, Morocco; Otmane Raji Otmane.raji@um6p.ma Geology and Sustainable Mining, Mohammed VI Polytechnic University, Benguerir 43150, Morocco

et al., 2021; El Desouky et al., 2010; Muchez et al., 2015). Sometimes, the BSR and TSR processes could act together as is the case for the Neoproterozoic Katanga Supergroup (El Desouky et al., 2010; Muchez et al., 2015).

Several deposits of native sulphur have been reported in the Mediterranean region (Figure 1). They occur mainly interbedded in Miocene evaporitic sediments and limestones or as sulphur nodules enclosed in secondary gypsum or carbonate deposits. The most studied occurrences include Teruel, Hellin, Lorca, Las Minas and the Granada basins in the eastern and southeastern Spain (Andreetto et al., 2019; García-Veigas et al., 2015; Lindtke et al., 2011; Ortí et al., 2010; Pineda et al., 2021), and those of the Messinian succession of Sicily and Northern Apennines in Italy (Caruso et al., 2015; Rossi et al., 2021; Ziegenbalg et al., 2010). Over the past decade, research interest in these deposits has been largely driven by their scientific value and significant progress in the analysis of molecular fossils and isotopic geochemistry leading to a better understanding of their genesis and paleoenvironmental conditions.

In northern Morocco, the Rif domain includes several Neogene basins resembling those that host native sulphur deposits in Spain and in Italy, in terms of geological setting and lithological facies. They notably show large gypsiferous marl, carbonate, and organic matter-rich deposits (Achalhi et al., 2016; Sani et al., 2000). However, until now, no available study has addressed the presence of native sulphur in this area. This study discusses for the first time the potential of Miocene sedimentary sequences in northern Morocco to host native sulphur deposits. For this purpose, two basins were selected and studied by combining field descriptions of lithostratigraphical facies with mineralogical and geochemical characterisation. Their potential to host native sulphur was discussed based on known indicative geo-markers, and on comparisons with similar contexts in the northern Mediterranean domain, mainly the southeastern Spanish basins where native sulphur occurrences were reported.

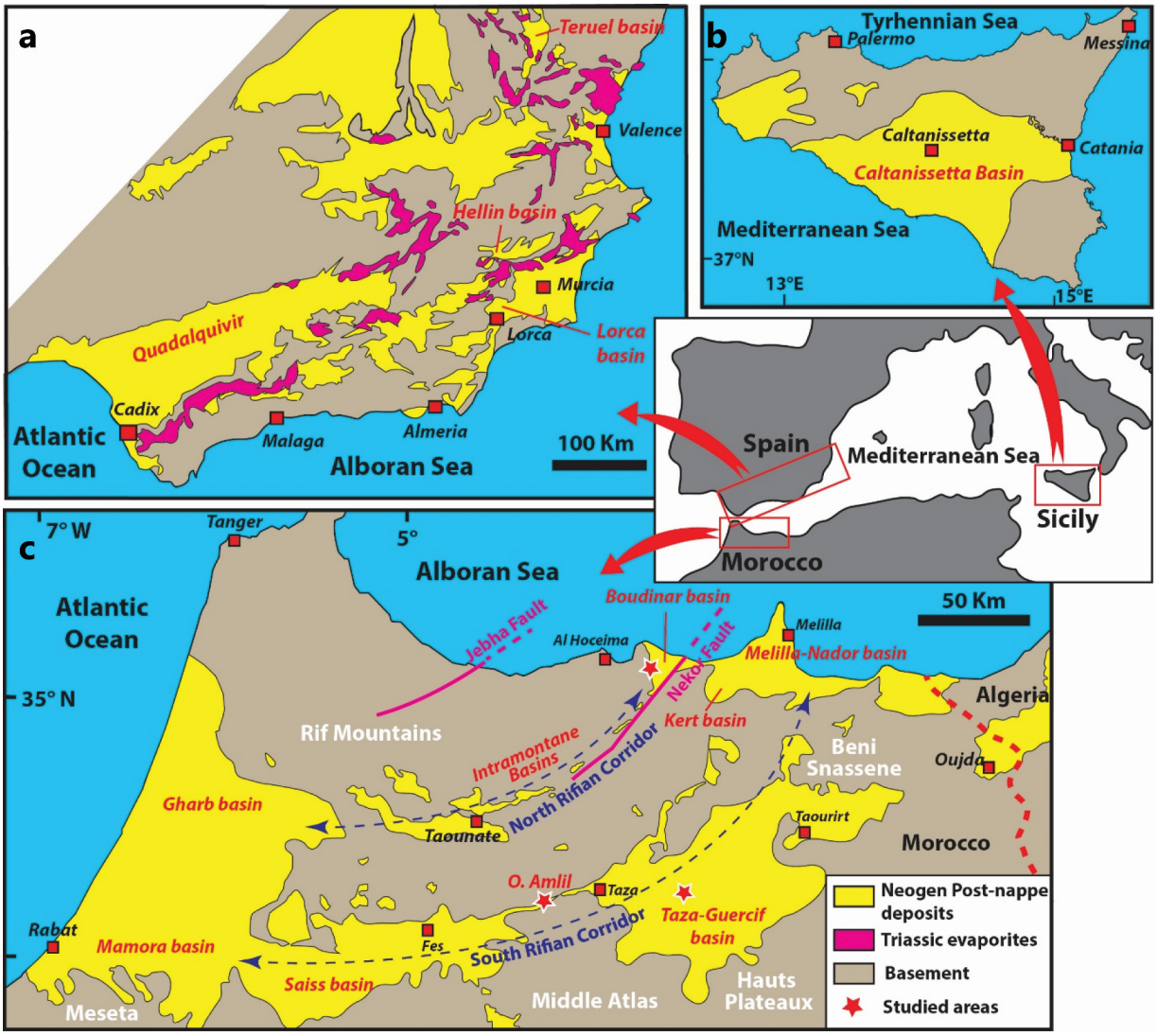

Figure 1. Simplified geological maps of (a) Southeastern of Spain (modified after Andreetto et al., 2019; Carpentier et al., 2020), (b) Sicily (modified after Butler & Lickorish, 1997 and (c) Moroccan Rif (modified after Capella et al., 2018).

2. Geological and stratigraphic setting

The Rif belt in Northern Morocco and the Betic Cordillera form the westernmost termination of the Alpine-Himalayan orogenic system (e.g. Platt et al., 2013). It includes several units, such as the Internal Zones, the Flysch Units, and the External Zones (e.g. Iribarren et al., 2009 and references therein). These units have been influenced by the convergence of Tertiary compression and subsequently by the pervasive extensional event since the early Miocene (Jolivet & Faccenna, 2000; Platt et al., 2013). In this regional context, Neogene post-nappes basins that initially formed the Rifian Corridors were individualised in response to an E-W extension during Tortonian (Achalhi et al., 2016; Brahim & Chotin, 1989; Iribarren et al., 2009; Krijgsman et al., 1999). In northern Morocco, they include the basins situated between the Boudinar and Gharb basins from the North Rifian Corridor and those located between the Melilla-Nador, Saïs, and Mamora basins originated from the South Rifian Corridor (Figure 1). The Boudinar and Taza-Guercif constitute key basins of the Rif as they have been situated along Corridors of the orogen (Figure 1). Tectonic processes combined with climatic and eustatic changes lead to the progressive restriction and closure of these gateways (Pérez-Asensio et al., 2013 and references therein). Subsequently, the Mediterranean Sea and the peripheral basins evolved into evaporitic basins during the so-called Messinian Salinity Crisis (Roveri et al., 2014).

The Boudinar basin of the North Rifian Corridor is located in the eastern part of the Rif region (Figure 1) and developed on a basement composed of Cretaceous metamorphic nappes or Neogene volcanics of the Ras-Tarf massif (e.g. El Azzouzi et al., 2014). Several works have described the lithostratigraphical sequence of this basin (Achalhi et al., 2016; Cornée et al., 2016; Merzeraud et al., 2019). Its Neogene sedimentary record starts with Early Tortonian continental conglomerates and lagoonal sandy marls -Unit I- (Achalhi et al., 2016). The second unit consists of a marine conglomerate, sandstone, and a thick (150 m) marine marls with several interbedded volcanic tuffs (dated ca. 10 – 7 Ma) and limestones (Subunit IIa); Late Tortonian (e.g. Achalhi et al., 2016). The Late Miocene succession of the basin ends with a thick (40 m) marine marl sequence with several interbedded diatomite layers (Subunit IIb; Early Messinian; Achalhi et al., 2016). The top of Unit II is truncated by the Messinian Erosional Surface and covered by thick continental conglomerates with gypsum olistoliths (Late Messinian; Cornée et al., 2016) and then by thick (up to 150 m) Early Pliocene marine sandy marls (Merzeraud et al., 2019). In addition, hydrothermal alteration zone is observed within the volcanic massif of Ras Tarf in the western edge of the basin (Choubert et al., 1984). Triassic evaporites (gypsum) outcrops to the south of the basin and along the Nekor fault in the Taghzout Tassa and Arbaa Taourirt areas.

The Taza-Guercif basin of South Rifian Corridor is located in the foreland of the eastern part of the Rif (Figure 1). The Palaeozoic rocks form the main basement of the basin covered first by a Permo-Triassic continental sequence (including red marls, evaporites, and basalts), and then by Jurassic dolomites, limestones, and marls (Bernini et al., 1999; Pratt et al., 2016). The Neogene deposits of the basin consist of five lithostratigraphic units separated by a tectonic unconformity (El Kati et al., 2017; Felletti et al., 2020; Krijgsman et al., 1999). The first continental sequence ('*Draa Sidi Saada Formation*') is made up of conglomerates and red silty-marls (Serravallian-Middle Tortonian), progressing towards the transitional and shallow-marine sequence of *'Ras el Ksar Succession'* (conglomerates, sandstones, and marls); Upper Tortonian (Felletti et al., 2020; Krijgsman et al., 1999) and the deposition of an open-marine sequence of *'the Melloulou Succession'*. This is overlain in turn by the transitional and continental deposits of the *'Kef ed Deba'* (including Lower Messinian marls and sand), then by continental conglomerates and lacustrine limestones of the '*Bou Irhardaiene*' formations of Upper Messinian to Plio-Quaternary (Bernini et al., 1999; Krijgsman et al., 1999). The Melloulou Succession shows interesting formations composed mainly of blue marls, turbidites, and gypsiferous marls, which are well exposed between the Melloulou and the Zobzit Rivers (Bernini et al., 1999; Felletti et al., 2020; Pratt et al., 2016). In addition, this Melloulou succession offers an effective seal for potential hydrocarbon deposits of the Jurassic carbonates (Bernini et al., 1999; Felletti et al., 2020; Pratt et al., 2016).

3. Material and methods

A detailed facies analysis has been carried out on three continuous and complete stratigraphic sections (Table 1): (1) Guercif section (34,030768°N; 3,741,709°W), (2) Taza-Oued Amlil section (34,179,084°N; 4,314,417°W) and (3) Boudinar Moulay El Arbi section (35,209,122° N; 3,682,421°W). Their descriptions include lithology, texture and geometry of sedimentary bodies, facies and sedimentary structures.

The facies of interest were sampled systematically at each outcrop for petrological analysis (Table 1). Thin sections were prepared and examined using a standard microscope Leica DM2700P in the Geo-Analytical Lab of the Geology and Sustainable Mining department at Mohammed VI Polytechnic University (UM6P, Benguerir, Morocco). The mineralogical composition of selected samples was determined by X-Ray diffraction on a Bruker D8 Advance using Cu Kα radiation

Table 1. Overview on the studied Neogene deposits for mineralogical and geochemical analysis.

Locality	G. Coordinate	Sample	Comment
Guercif	34.030768°N	Gr01	Lignite
	3.741709°W	Gr03	Yellow facies nodule
		Gr04	Yellow facies nodule
Taza-Oued Amlil	34.179084°N	Am01	Salt dome
	4.314417°W	Am02	Lignite
		Am03	Yellow facies nodule
		Am04	Yellow facies nodule
		Am06	Yellow facies nodule
Boudinar Moulay El Arbi	35.209122°N	Bd02	Yellow facies
	3.682421°W	Bd04	Yellow facies
		Bd06	Yellow facies

(1.5418 Å) T 40Kv and 40 mA at the UM6P laboratory of Jorf Lasfar (El Jadida, Morocco). The sample powders were scanned over a diffraction angle (2θ) ranging between 5° and 70° with a step size of 0.01°, a time step of 1 s, and 15 min of acquisition time. The X'expert Highscore Plus with the open crystallography database (COD 2021; Vaitkus et al., 2021) was used to identify and quantify the major existing phases in the samples, with detection limit of 1–5%. Whole-rock major element compositions were obtained by X-ray fluorescence (XRF) using a PANalytical Epsilon 4 spectrometer at UM6P. Carbon and sulphur contents were determined using ground and homogenised bulk solid samples analysed by a LECO CS 300 CS-Analyser at UM6P.

4. Results

4.1. Stratigraphy and facies description

4.1.1. Guercif

The studied section started in the banks of the Khendek el Ouaich river (Figure 1). This area exposes about 20 m thick succession consisting of gypsiferous marls followed by white cinerites with gastropods, alternating with lignite and clayey marls units (Figure 2(a,c)). The cinerite levels come from the Guilliz volcano dated at 7.4 Ma (Choubert et al., 1968). Magnetostratigraphic data performed on this succession (El Kati et al., 2017), which is part of the *'Mellelou formation'*, indicate an Uppermost Tortonian age. Micro-fauna assemblages in these deposits refer to a lagoonal and lacustrine environment (Colletta, 1977). This first succession is stratigraphically overlaid by thick gypsiferous marls (Figure 2(a,b)) of the Messinian *'Mellelou formation'*. The selected facies as of interest in this section are present in the Early Messinian gypsiferous marls (Figure 2(b)), and they correspond to sub-spherical concretions or nodules reaching 50 cm in diameter. They occur as yellowish fine-grained sediment associated with gypsum and iron oxides (Figure 2(d)) that appear dispersed at different levels (Figure 2(b)). The core of these nodules is composed mainly by gypsum surrounded by yellowish fine-grained sediment and subsequently by gypsum and iron oxides (Figure 2(d,e)). Other facies of interest are found within the gypsiferous marls as gas escape features (Figure 3(a,b)). They consist of concentric pipe-like structures of silicified marls with gypsum and iron oxides (Figure 3(c)). Felletti et al. (2020) interpreted these structures in the Guercif basin as a concretion of authigenic carbonates developed around a conduit filled with sulphur-bearing minerals.

4.1.2. *Taza*-Oued Amlil

The section crops out at 5 km east of the Oued Amlil village and at 20 km west of Taza city (see location in Figure 1). It is about 30 m thick and shows an Upper Miocene succession of grey marls and organic matter-rich dark marls (Figure 4(a, b)). The sequence can be subdivided in two distinct units: (i) the lower unit consists of 13 m-thick dark marls, containing lignite beds (Figure 4(f, g)) intruded by a salt diapir of Triassic age according to; Figure 4(h)). The upper unit consists of 14 m thick grey marls. The facies of interest take the form of nodule structures (5 to 30 cm in diameter) within the lignite beds and the top of the grey marls (Figures 4(c,d,f)). These nodules show gypsum in its core surrounded by yellowish colour fine-grained sediments, then by gypsum and iron oxides in the extern part (Figure 4(c–e)). Some of them show quite a resemblance with those found in the Guercif section with a concentric structure starting with gypsum in the nodule core followed by yellowish fine-grained sediments surrounded by gypsum and iron oxides (Figure 4(d)). Nodules associated with lignite and organic-rich marl unit are surrounded by gypsum, yellowish sandy marls and iron oxides.

4.1.3. Boudinar Moulay El Arbi

The Moulay El Arbi section is located in the Western part of the Boudinar basin (near the Ras Tarf Volcanic Massif; Figure 5(a)), attaining a thickness of about 100 m. The studied section (Figure 5(b,c)) corresponds to the second sedimentary unit (Unit II) of the Tortonian-Early Messinian age, as described by Achalhi et al. (2016). It is mainly formed by grey and yellow silty marls that are interbedded with white volcanic tuff layer (Figure 5 B). The facies of interest are present at the top and bottom of the tuff level (Figure 5(b,d)). They consist of a complex arrangement of yellowish fine-grained sediment associated with organic-matter-rich clayey marls, gypsum, and iron oxides. The yellowish lithologies show diversified morphologies, ranging from lenses (>10 cm in length), and centimetric laminae to very irregular masses arranged parallel to the stratification (Figure 5(d)). They also take the form of cone-shaped concretions over the volcanic tuffs and gypsum crystals (Figure 5(e)).

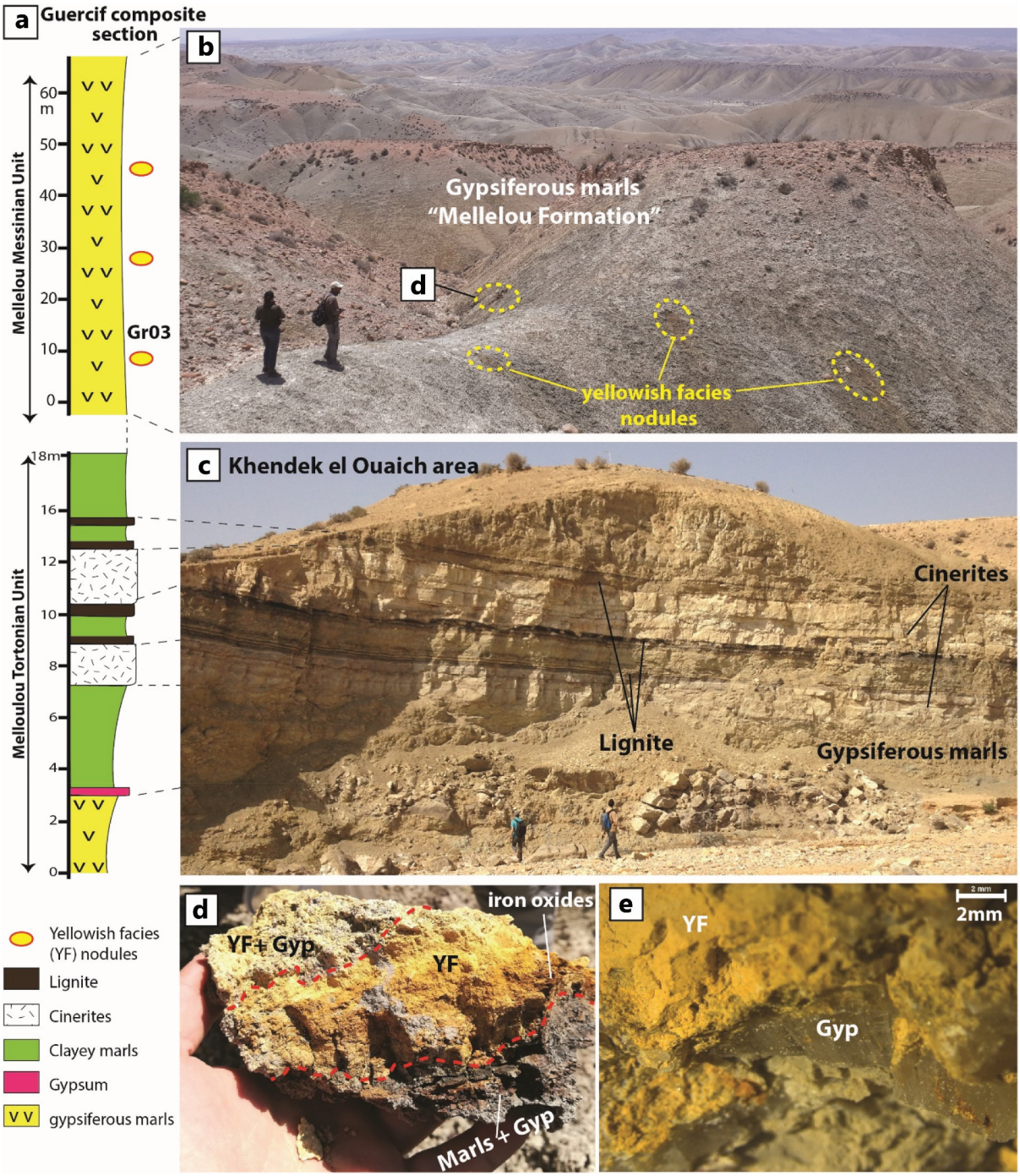

Figure 2. (a) Stratigraphic column of the Guercif composite section. (b) Field overview of the Miocene 'Gypsiferous Marls' of the Melloulou Formation from the Taza-Guercif basin showing scattered large yellowish facies nodules. (c) Field overview of the Latest Tortonian–Earliest Messinian lacustrine deposits in the Khendek el Ouaich area (Taza-Guercif basin). (d) Detailed view (hand specimen) of the yellowish-facies nodules associated with gypsum and iron oxides. (e) Microphotography showing the gypsum-yellowish facies association. YF: Yellowish facies; Gyp: Gypsum.

4.2. Petrographic characterisation

Thin sections of the lignite sample Am02 collected in the Taza-Oued Amlil area (see the stratigraphic location in Figure 4) show the presence of dark organic matter with impregnations of pyrite microcrystals (Figure 6(a,b)). Porosity is filed by a mixture of yellowish-brown cryptocrystalline assemblage with a mosaic-like structure (Figure 6(a,b)) and large scattered automorphic pyrite and zoned dolomite crystals (Figure 6(b,g)). Pyrite grains range between 5 µm to 1 mm in size and appear disseminated in the section. They show automorphic cubic, spherical and framboidal habit, usually surrounded by a corona of iron oxides (Figures 6(d–f)). The yellow cryptocrystalline assemblage displays different textures; the first one of bright yellow colour occupies the core of the porosity of the organic matter, surrounded by the second one that appears like a mosaic or cluster of yellow-

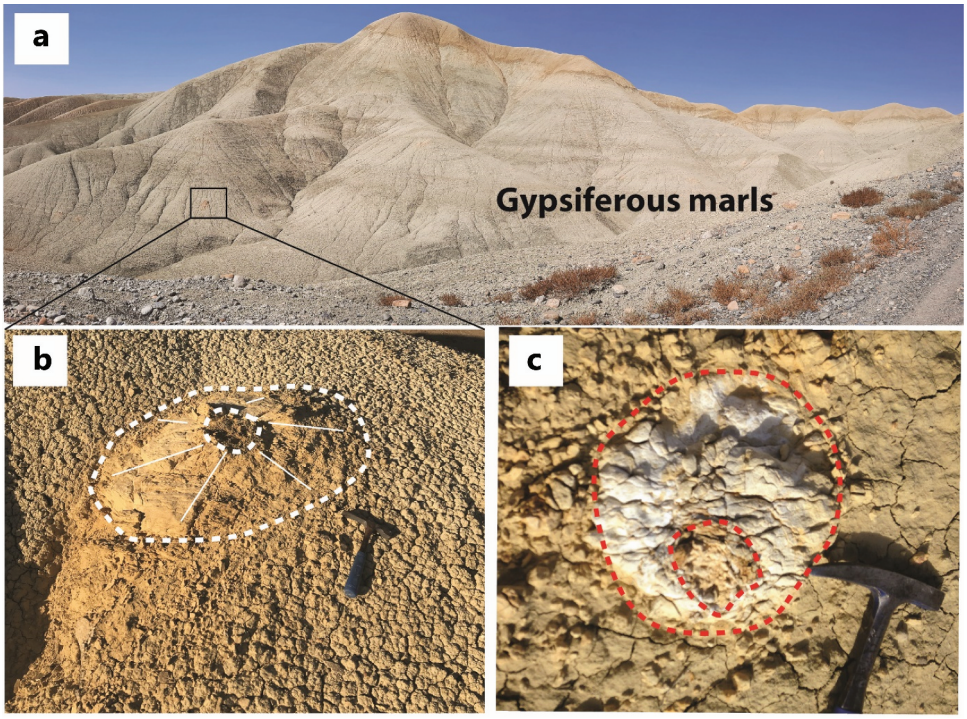

Figure 3. (a) Field view of the Miocene gypsiferous marls from the Taza-Guercif basin displaying gas escape structures. (b) Field view and aspect of the gas escape features showing a fumarolic-like structure. (c) Detailed view of silicified marls within the gas escape features.

brown colour grains (Figure 6(a,b)). The Am02 thin-section show also a carbonate articulated alga (Figure 6(h)), microbial crusts, crustacean coprolite and zoned dolomite grains which indicate a reducing environment. In the yellowish facies nodules, thin section of the Am04 sample (see stratigraphic position in Figure 4) show the abundance of large (1 to 5 mm) sub-automorphic gypsum crystals, surrounded by a mixture of minerals composed of automorphic zoned dolomite, pyrite, detrital quartz and feldspar particles, calcite and muscovite (Figure 6(c)). Pyrite disseminated in the section shows a globular form encrusted by iron oxides (Figure 6(c)).

Sample Gr03 collected in Guercif area (see stratigraphic position in Figure 2) show similar structure and mineralogical assemblages as the Am04 sample (Figure 7(a)). It consists of large gypsum crystals with microfractures filled by bright yellow matter (Figure 7(a)) surrounded by a mixture of bright yellowish and brown cryptocrystalline assemblage and scattered microcrystals of partly oxidised pyrite (Figure 7(b)). In contrast, the Boudinar sample BOD02 shows a crust-like structure of yellowish-brown cryptocrystalline assemblage over the white volcanic tuffs (Figure 7(c,d)). The yellowish-brown cryptocrystalline assemblage shows a mosaic-like microstructure with bright yellow minerals in the cores surrounded by the brown mineral on the edges (Figure 7(d)). We also note the abundance of detrital quartz and disseminated pyrite (Figures 7(c,e,f)).

4.3. Mineral and major-element bulk analysis

The XRD patterns of the selected samples are displayed in Figures 8 and 9. These samples correspond to the facies of interest described above as mainly yellowish sandy masses associated with gypsiferous marls (see, Table 1). They revealed a mineralogical assemblage composed mainly of gypsum, jarosite, and quartz. As accessory minerals, they contain a variety of minerals, such as iron oxides (mainly goethite), carbonates (mainly calcite), and silicates (mainly clay). Native sulphur occurs in significant amounts in sample AM04 from the Taza-Oued Amlil section. In the other samples, native sulphur is not detectable, probably due to the alteration. In terms of elemental contents (Table 2), the whole-rock XRF analysis show that SiO_2 (18–24 wt.%.), CaO (12–30 wt.%.) and total Fe_2O_3 (5–16 wt.%.) as well as total sulphur (18–45 wt.%, expressed as sulphur oxides SO_3) represent the most abundant elements. These contents reflect the mineralogical composition and show that the sulphur from the studied samples is mainly associated with gypsum and/or jarosite except for the samples AM04 whose CaO content does not exceed 9 wt.% and the Fe content of 14 wt.%.

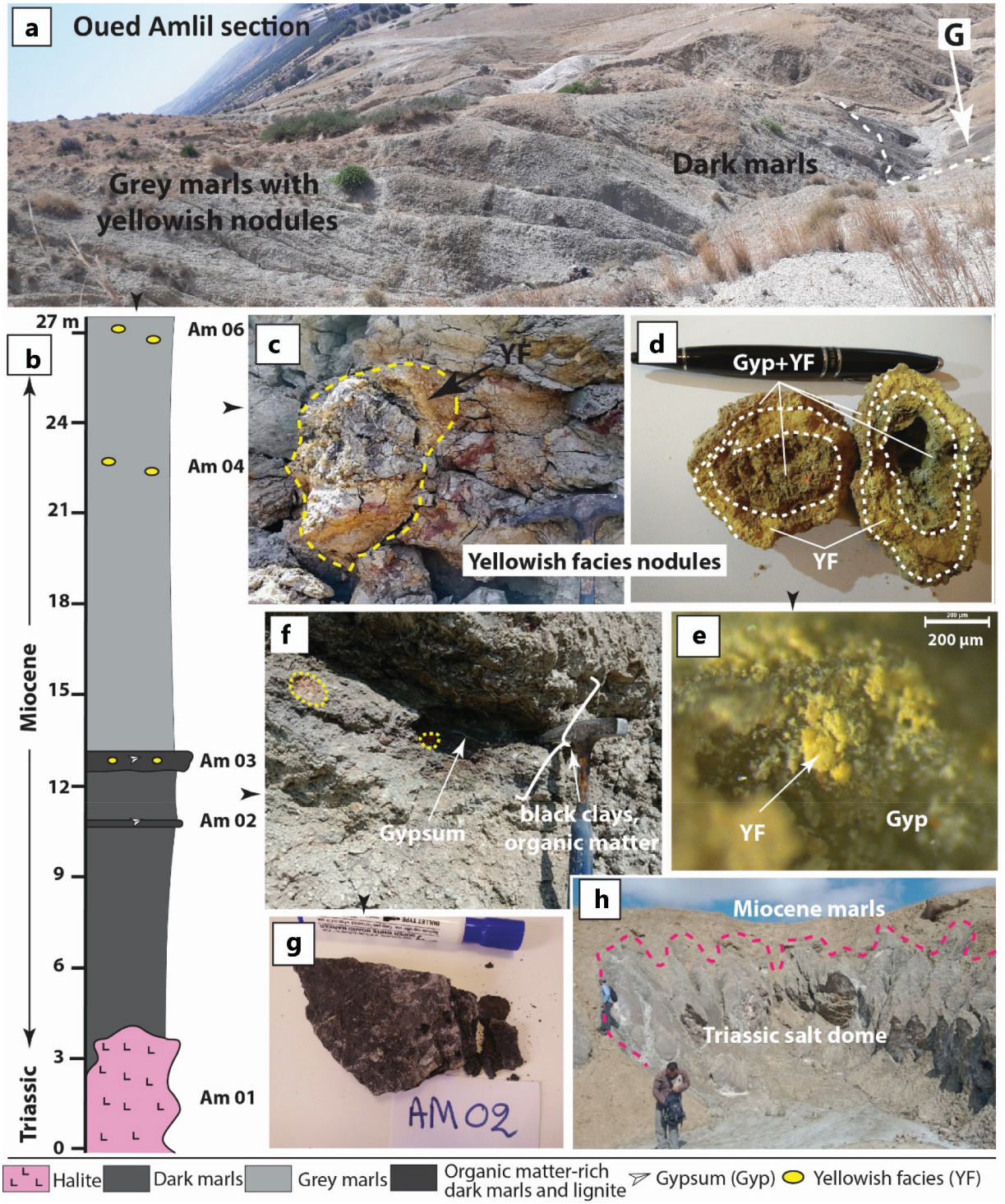

Figure 4. (a) Field overview of the Miocene deposits at the Taza-Oued Amlil area. (b) Stratigraphic column at the Oued Amlil area. (c, d) Detailed view of the yellowish-facies nodules from the upper part of the section, composed of gypsum, yellowish facies and iron oxides. (e) Microphotography showing the gypsum-yellowish facies association. (f, g) Detailed view of the organic matter-rich facies (lignite) associated with the basal dark marls. (h) Triassic salt dome outcropping in the base of the Oued Amlil section.

5. Interpretation and discussion

5.1. Stratigraphic correlation with Neogene basins from Spain and Sicily

Similar to other Rifian Neogene basins, the two studied basins (Boudinar and Taza-Guercif basins) show geological setting and several features comparable to their counterparts in the Betic region, Southern Spain (Figure 1), which are well known for hosting native sulphur deposits (e.g. Lindtke et al., 2011; Ortí et al., 2010). The Betic occurrences consist of intermontane and marginal basins, located mainly in the External Zones of the Betic chain and characterised by either marine or lacustrine sedimentation (Figure 1, Table 3). In the Teruel lacustrine basin (NE Spain), native sulphur concentrations occur within the Tortonian *'Libros Gypsum'* formation (Figure 10; e.g. Ortí et al., 2010). Host sediments consist mainly of lacustrine gypsum and limestones with lignite

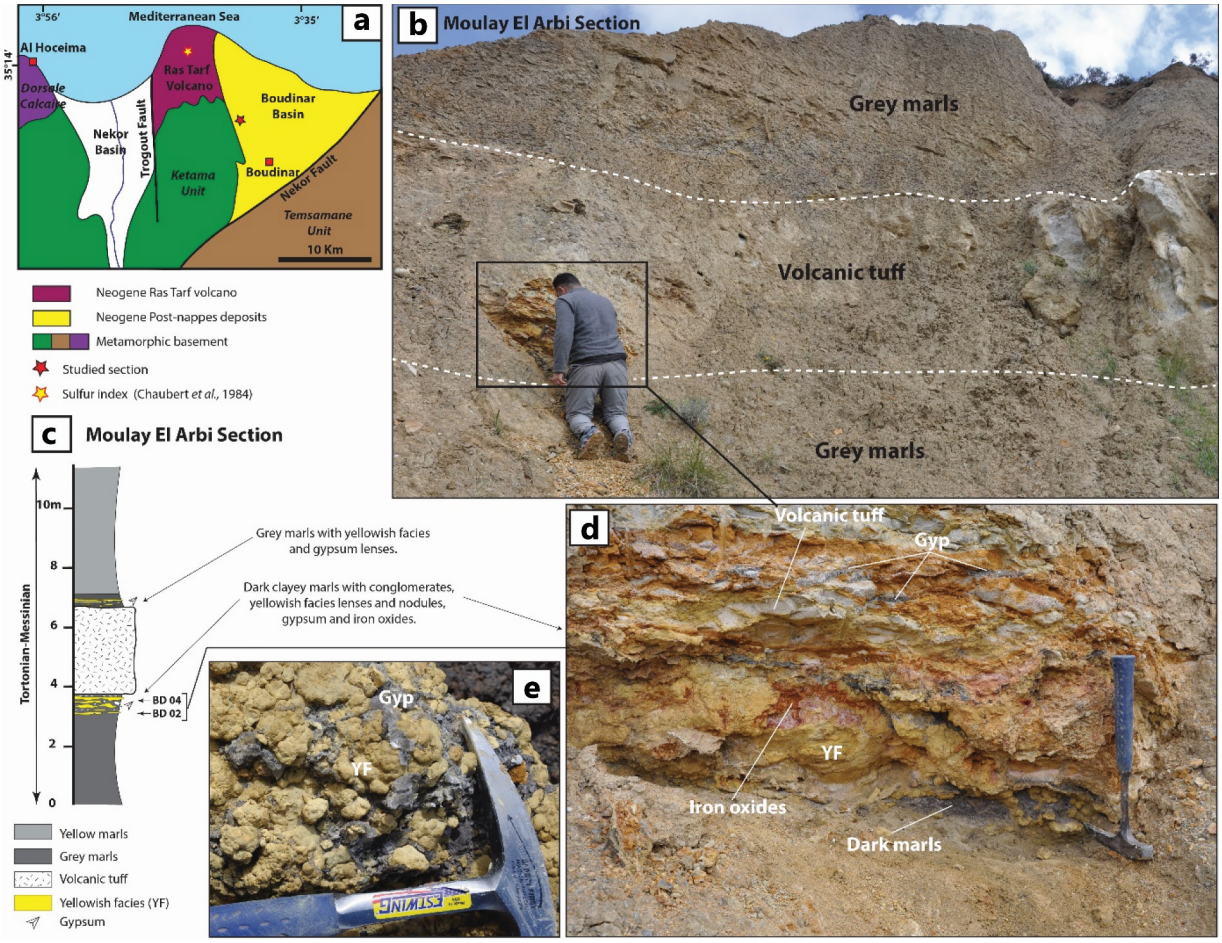

Figure 5. (a) Simplified geological map of the studied Boudinar area. (b) Overview of the interbedded volcanic tuff in the Tortonian marls showing yellowish facies at the bottom of the volcanic tuff. (c) Stratigraphic column of the *Moulay El Arbi* section. (d) Detailed view of the yellowish facies associated with gypsum, volcanic tuff, iron oxides and dark clayey marls. (e) Yellowish facies concretions associated to gypsum and dark clayey marls.

beds corresponding to the *'Bituminous-Calcareous'* and *'Gypsum'* subunits (Figure 10, Table 3; Anadón et al., 1992; Ortí et al., 2010). These units can be correlated with similar lacustrine deposits described in this study from the Uppermost Tortonian succession in the Khendek el Ouaich area of the Taza-Guercif basin (Figure 2). In the latter, lacustrine carbonates, lignite, and cinerites alternating with gypsiferous marls are evidenced. However, no pure evaporitic deposits occur in this sequence, where only gypsiferous marls are observed. Such paleoenvironmental change to a lacustrine setting in the uppermost Tortonian can be compared with a similar change observed in the Hellín basin (Spain, see location in Figure 1(a)). In the latter, the Neogene succession consists mainly of Middle Tortonian marine marls with interbedded limestones and diatomites (Calvo et al., 1978), passing upward to the thick-lacustrine gypsum and carbonate deposits of the *'Las Minas de Hellín Formation'* of Late Tortonian age (Servant-Vildary et al., 1990). Sulphur-bearing carbonate strata (mainly diagenetic dolomite) and abundant nodules of native sulphur occur in the laminated gypsum, carbonate beds and marlstone layers of the *'Las Minas de Hellín Formation'* (Lindtke et al., 2011).

In the Spanish marine Lorca basin (see location in Figure 1(a)), the Upper Miocene deposits consist of Serravallian sandstones and conglomerates (*'Soriana Formation'*), Tortonian marine marls (*'Hondo Formation'*) and Messinian marls with interbedded diatomite layers ('*Tripoli Formation*'; Andreetto et al., 2019; Carpentier et al., 2020; Rouchy et al., 1998; Sælen et al., 2016). Sulphur-bearing limestones are interbedded within the alternation of marls and diatomaceous layers of the *'Tripoli Formation'* (Andreetto et al., 2019; Rouchy et al., 1998; Figure 8). This formation can be correlated with the Messinian Sub-Unit IIb of the Boudinar basin (Northern Morocco), also displaying diatomaceous layers (Figure 10; e.g. Achalhi et al., 2016). It may also be correlated with the Messinian Melloulou *'Gypsiferous Marls'* formation of the Taza Guercif basin (South Rifian Corridor), in which we identified sulphur/jarosite nodules.

In Spain, most Neogene basins hosting native sulphur (e.g. Teruel, Hellín and Lorca basins) are partly developed on a Triassic basement with evaporites (gypsum and salt; Table 3, Figure 1). A similar setting is observed in Morocco, where the Rifian counterparts of the Spanish occurrences were developed on Triassic evaporitic formations – or in close vicinity. In addition, similar to the

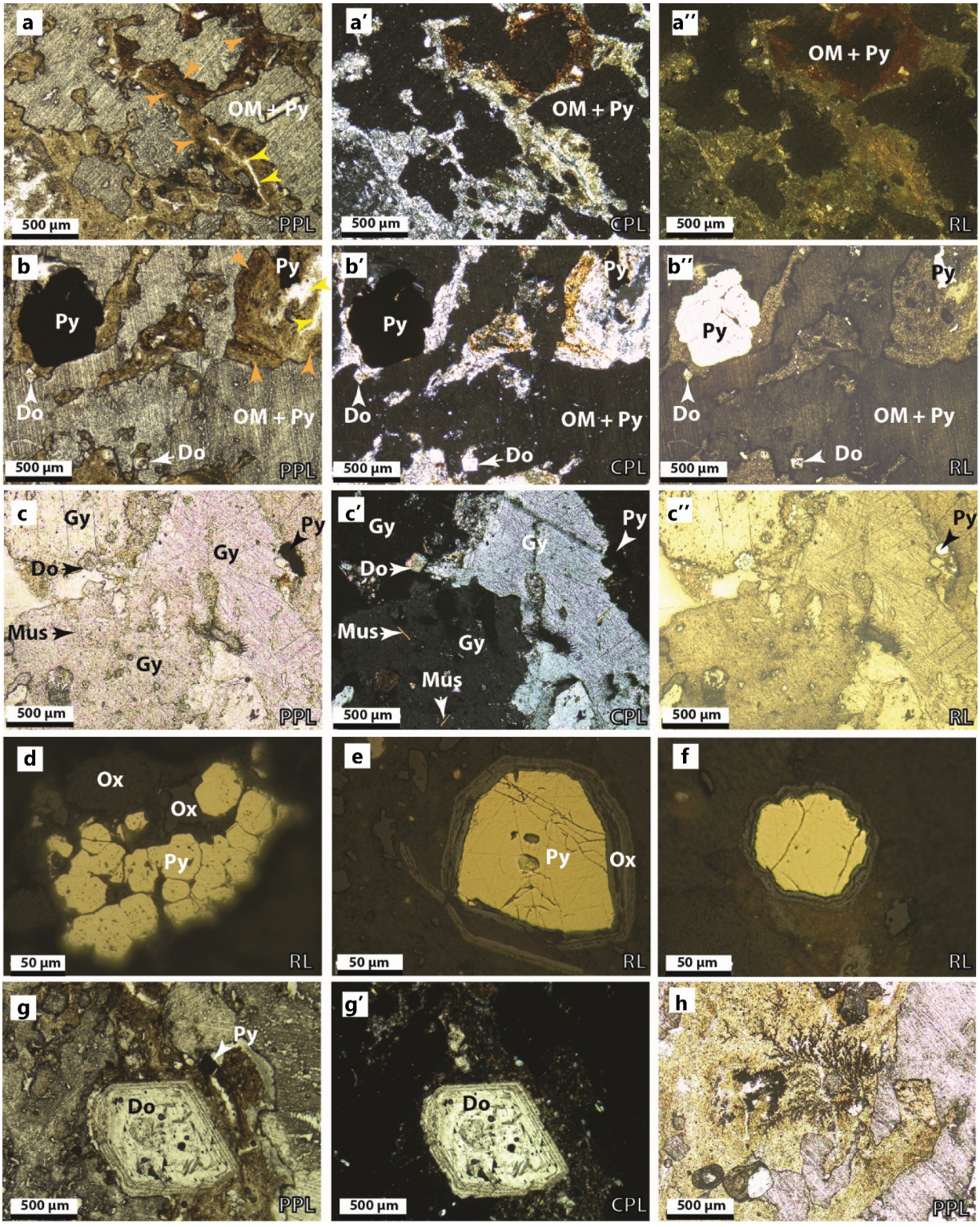

Figure 6. Thin sections of the Am02 lignite and Am04 yellowish nodules samples (see stratigraphic position in Figure 4). a, b) Optical photomicrographs of Am02 thin-section showing dark organic matter (OM) with impregnations of pyrite (Py). The spaces between the organic matter are filed by a mixture of yellowish-brown minerals (Orange and yellow arrows), pyrite and dolomite (Do) crystals. (PPL: plane polarised light; CPL: cross polarised light; RL: Reflected-light). c) Optical photomicrographs of Am04 thin-section showing large sub-automorphic gypsum crystals (Gy) surrounded by a mixture of minerals composed of automorphic zoned dolomite, circular pyrite, calcite and muscovite (Mus). d, e, f) Detailed photomicrographs of pyrite crystals from Am02 sample showing a globular form surrounded on the edges by iron oxide crusts (Ox). g) Detailed photomicrographs of zoned dolomite crystals from the Am02 thin section. h) Detailed photomicrographs of articulated algae from the Am02 thin section.

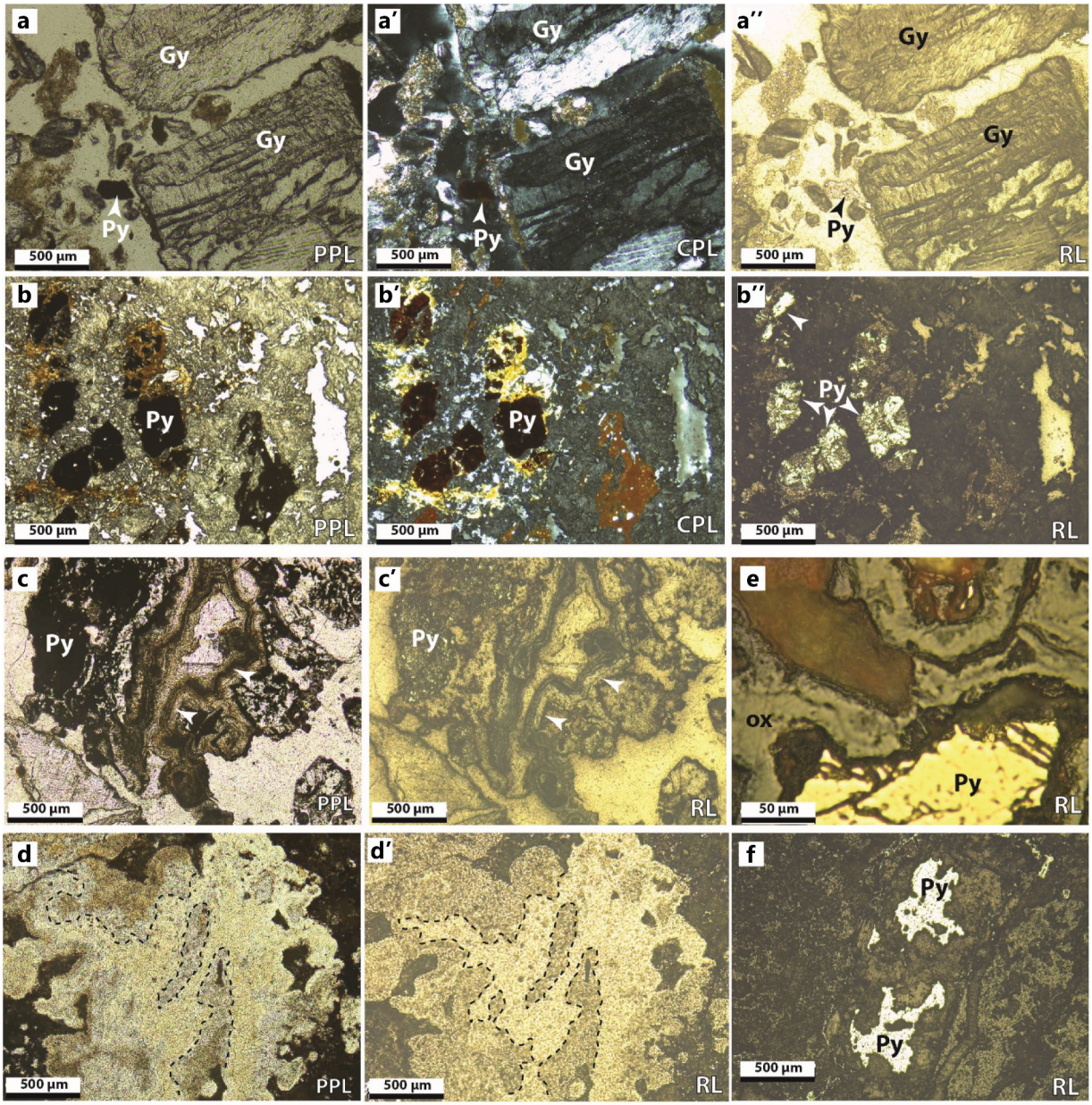

Figure 7. Optical photomicrographs from thin sections of the Gr03 yellowish nodules and Bd02 samples (see stratigraphic position in Figures 2 and 5). (a) Large sub-automorphic gypsum crystals surrounded by a mixture of yellowish minerals and pyrite (Gr03). (b) Pyrite minerals replaced on the edges by yellowish-brown minerals and iron oxides (Gr03). (c) Bd02 thin section showing pyrite minerals and yellowish-brown minerals crusts over the white volcanic tuffs. (d) Bd02 thin section showing yellowish minerals crusted by brown mosaic-like minerals. (e, f) Detailed photomicrographs of pyrite minerals replaced by iron oxides (Bd02).

sedimentary series around the Teruel basin (Servant-Vildary et al., 1990), the studied Taza-Oued Amlil area is associated with Triassic salt domes (Figure 4).

In contrast, native sulphur occurrences in the Caltanissetta basin (Central Sicily, Figure 1) are associated with diagenetic limestone (*'Calcare Solfifero'* subunit) and intercalated in the Messinian evaporites (*'Formazione Gessoso–Solfifera'*) resulting from the Messinian Salinity Crisis (Butler et al., 1995; Decima et al., 1988; Oliveri et al., 2010; Ziegenbalg et al., 2010). It is worth mentioning that the Messinian evaporite deposits are missing in the Neogene post-nappes basins of Northern Morocco. They were mostly eroded in the Boudinar Basin and are only recorded as olistoliths over the Messinian Erosional Surface (Cornée et al., 2016).

5.2. Forming process of the native sulphur

Our field observations of the Neogene Moroccan basins combined with mineralogical and geochemical characterisation, reveal several facies that can be considered as hints of sulphur-mineralising environments. Yellowish facies in the form of laminas, lenses or nodules characterised by mineralogical assemblages of jarosite, silica, pyrite and gypsum were found in different Miocene sedimentary sections (Figure 6–Figure 9). The yellow colouration is mainly due to the presence of jarosite, which is common in a variety of strongly acidic, sulphate-rich environments (Lueth et al., 2005; Martinez-Frias et al., 2006; Rodríguez & van Bergen, 2015; Whitworth et al., 2020).

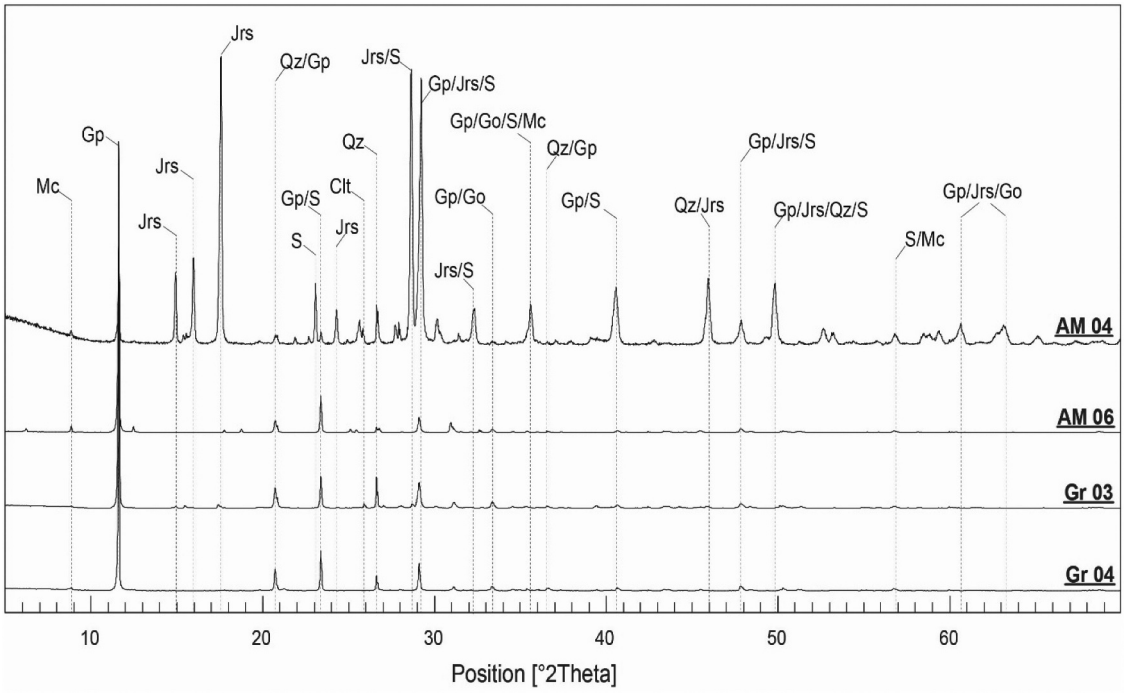

Figure 8. XRD patterns of the selected Taza-Guercif samples. Gypsum (Gp), sulphur (S), jarosite (Jrs), quartz (Qz), goethite (Go), mica (Mc).

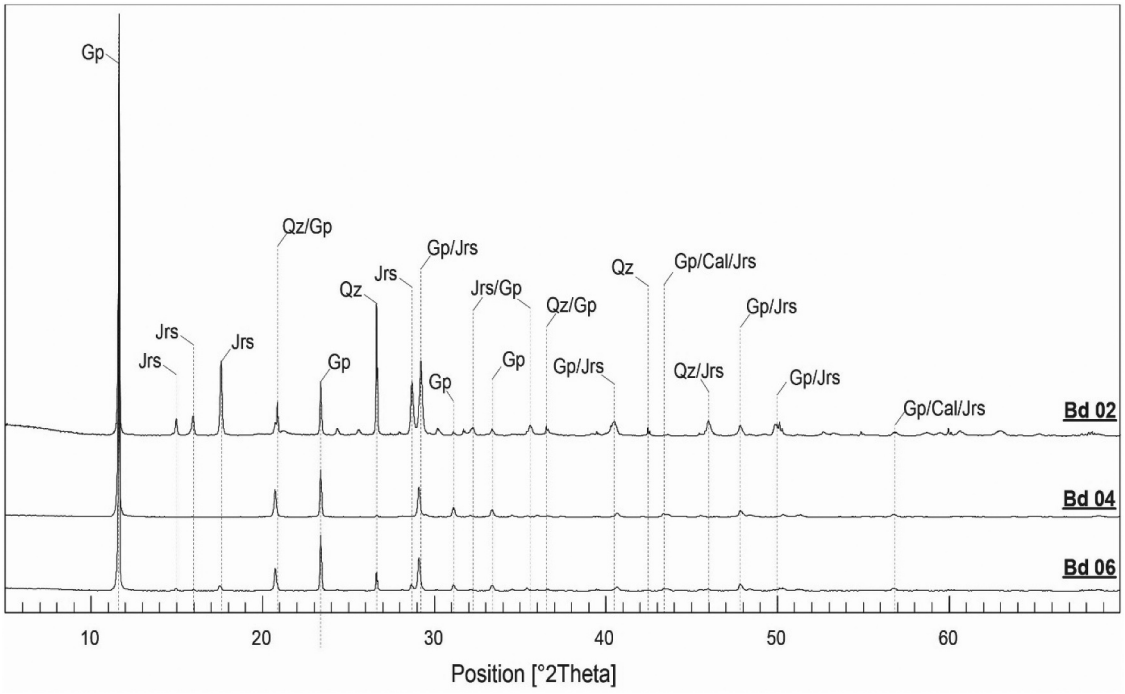

Figure 9. XRD patterns of the selected samples from Boudinar. Gypsum (Gp), jarosite (Jrs), quartz (Qz), calcite (Cal).

Table 2. Whole-rock major element concentrations (wt.%) of selected samples from the studied Guercif-Taza and Boudinar sections.

Sample	SiO_2	TiO_2	Al_2O_3	$Fe_2O_3^{tot}$	MgO	MnO	CaO	Na_2O	K_2O	P_2O_5	SO_3 (*)	CO_2 (*)	Total
Gr 03	24.5	0.29	3.83	5.85	0.69	0.01	15.9	0.45	1.65	0.13	28.87	0.22	82.43
Gr 04	18	0.21	4.35	15.23	0.91	0.04	16.8	0.69	0.87	0.14	18.36	0.95	76.60
Am 04	18.8	0.25	2.01	14.05	1.58	0.03	8.95	1.09	1.56	0.28	45.77	0.7	95.02
Am 06	9.28	0.14	2.95	1.57	3.19	0.02	25.9	0.05	0.29	0.42	38.15	3.67	85.63
Bd 02	14.5	0.19	5.42	11.62	0.42	0.01	16.9	0.18	1.29	0.32	24.57	0.44	75.84
Bd 04	2.76	0.05	0.7	0.4	0.37	0.01	31	0.07	0.09	1.01	42.90	2.64	81.99
Bd 06	14.6	0.24	2.92	8.06	0.12	0.01	20.4	0.16	0.77	0.3	26.94	0.33	74.87

*Analyses performed using Leco S/C analyser

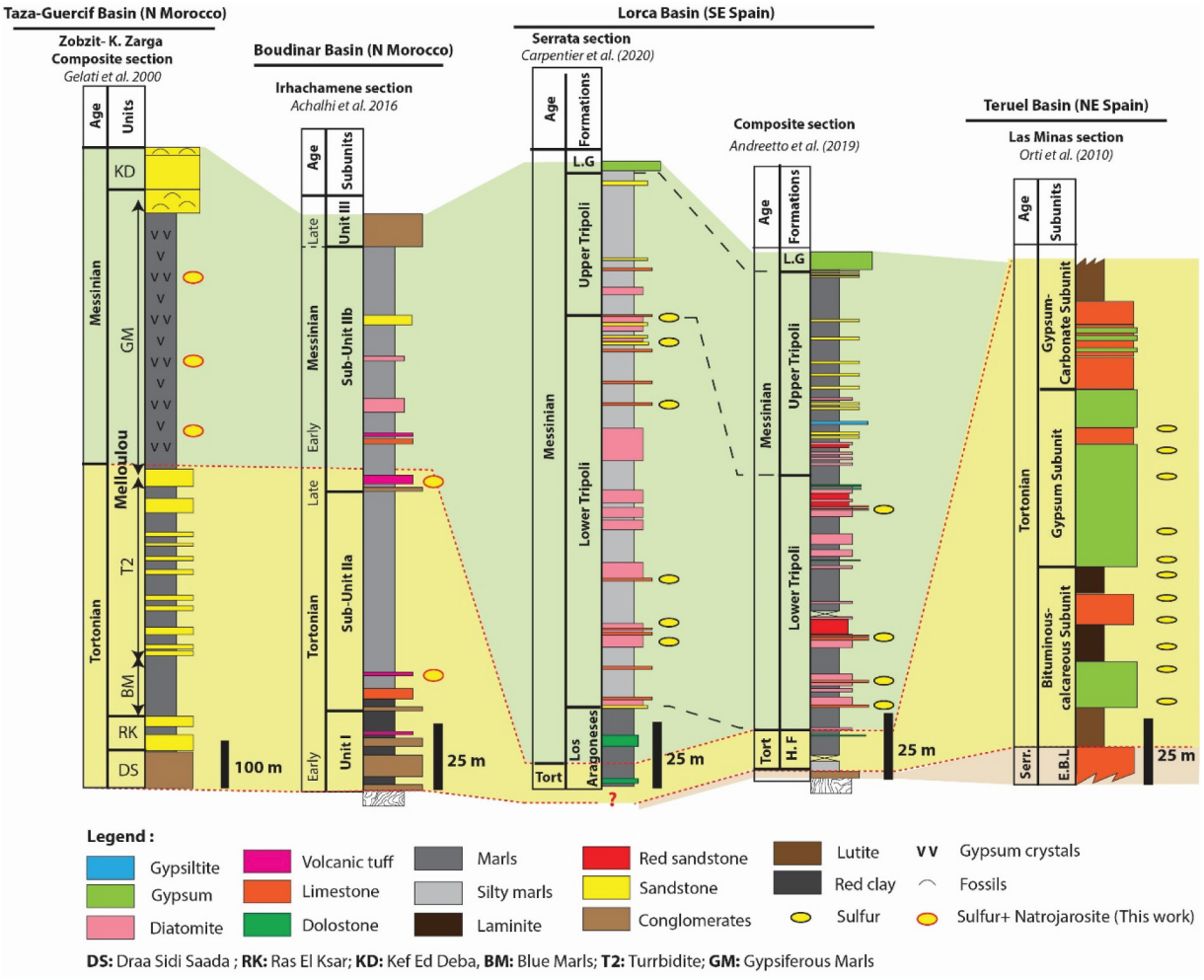

Figure 10. Stratigraphic columns of the Neogene basins hosting native sulphur from the northern edge of the Mediterranean Sea (SE Spain), correlated with the Boudinar and Taza-Guercif basins (N Morocco). Modified after Gelati et al. (2000); .Ortí et al. (2010), Achalhi et al. (2016), and Andreetto et al. (2019) and Carpentier et al. (2020)

According to Rodríguez and van Bergen (2015), volcanic hydrothermal systems can also produce jarosite- and gypsum-bearing assemblages near volcanic activity by the action of hot acidic fluids enriched in sulphur and halogens. Such a geological environment likely occurred in the Boudinar basin, which is located close to the andesitic Ras Tarf volcano emplaced in a subduction setting (El Azzouzi et al., 2014). The first eruptions of this volcano led to in-filling the Boudinar basin by stratified volcanic breccias deposited in submarine environment and interbedded with cinerites, both affected by pervasive hydrothermal alteration (El Azzouzi et al., 2014). In some cases, jarosite could be derived from the oxidation of iron sulphides in acid epithermal environments. Such origin was suggested by Martinez-Frias et al. (2006) for the Upper Miocene volcanism-related, hydrothermal suite of Jaroso unit (SE Spain), where the jarosite-gypsum assemblages are similar to those observed in the studied Boudinar basin (Figure 5). In most cases, however, jarosite has been considered to be derived from the supergene oxidation of iron sulphides that were originally present in the sediment (e.g. Whitworth et al., 2020; Znamenskiy, 1990). Diagenetic pyrite is commonly found in organic-rich sediments, where forms via bacterial sulphate reduction processes (Berner, 1970). This mineral was observed in all samples of the studied sections (Figures 6 and 7) and was previously described in the late Miocene marls of the Rifian Neogene basins (Amakrane et al., 2016). Pyrite represents a significant source of reduced sulphur and leaching by oxidising fluids can account for the formation of jarosite in near-surface conditions.

In contrast to the Boudinar basin, at the level of the Taza-Oued Amlil Miocene section, the presence of native sulphur associated with gypsum and pyrite is well observed. In this case, we postulate that the pyrite was formed in a first stage, as a result of sulphide production and reaction with sedimentary iron phases. Subsequently, jarosite and native sulphur were formed probably by bio-oxidation of pyrite (Karikari-Yeboah et al., 2019; Vithana et al., 2015). In these assemblages as can be observed in thin sections (Figures 6 and 7), gypsum may also represent a secondary phase formed

Table 3. A summary of the main stratigraphic features characterising the Neogene basins from the northern edge of the Mediterranean Sea (Spain and Sicily) where native sulphur occurrences have been reported.

Basin	Locality	Basement	Stratigraphy	Age	Native sulphur forms	host rocks	References
Hellin basin	External part of the Betic chains (SE Spain)	Cretaceous limestones and Triassic evaporites (gypsum and salt-domes)	Sedimentary record of the basin: - **'Marine Sequence' (Middle Tortonian)**: marine marls and marly carbonate beds (algal limestones) with diatomite in the upper part. - **'lacustrine sequence' (Late Tortonian)**: Thick gypsum and carbonate deposits of the *'Las Minas de Hellín Formation'*. overlain by carbonate. marls and diatomite. Several Triassic salt-domes appears in the sedimentary series all around the basin.	Middle to Late Tortonian	Native sulphur appears as: - spherical nodules in carbonate deposits. - Round aggregates in carbonate beds. -Amoeboidal aggregates. - tiny accumulations finely dispersed in the host rock.	laminated gypsum and dolomitic carbonate beds	- Lindtke et al. (2011) - Servant-Vildary et al. (1990) - Servant-Vildary. (1986)
Teruel basin	central part of the Iberian Chain (NE Spain)	Hercynian basement; Upper Triassic evaporites; Jurassic-Palaeogene cover (carbonates. mudstones. sandstones. and evaporites).	The Neogene sedimentary record of the Teruel basin consists of from base to top: - **'Lower alluvial unit'** (Aragonian): red alluvial deposits with gypsum intercalation in the upper part (El Morrón Gypsum). - **'The El Bolage Limestone'** (Aragonian): limestones with mudstones and lignites. - **'The Libros Gypsum'** (Vallesian): The Bituminous-Calcareous. Gypsum and Gypsum-Carbonate sub-units. - **'The upper alluvial unit'** (Vallesian-Turolian): red mudstones with interbedded sandstones. conglomerates and limestones. - **'The La Nava-Santa Bárbara Limestone'** (Turolian): massive limestones with interbedded carbonate mudstones. - **'Upper Turolian succession'**: Siliciclastic deposits. evaporites and lacustrine limestones.	Lower Miocene to Upper Pliocene	- Nodules. lenses or irregular masses. within the calcareous and carbonates beds. - thin levels. isolated nodules and lenses within the gypsiferous beds. - thin levels and small nodules within the marly laminite and oil-shale facies. - as a cement within carbonate and laminite layers.	Host rocks consist of gypsum; carbonates; marly laminite and oil-shale layers.	- Ortí et al. (2010) - Ortí et al. (2003) - Anadón et al. (1997)
Lorca basin	South-eastern Spain	Triassic formations (schists and evaporites)	The upper Miocene succession in this basin consist of: -**'Soriana Formation'**(Serravalian): sandstones and conglomerates - **'Hondo Formation'** (Tortonian): marine marls. - **'Tripoli Formation'** (Messinian): with two members. the lower one consists of marls and diatomaceous layers alternation. Six layers of sulphur-bearing limestones are interbedded in this lower member. The upper member composed of marls and sandstones. - **'Main Gypsum Unit'** (Messinian): with Two evaporitic units (Lower and Upper) consisting of gypsum and halite.	Tortonian / Messinian	Dense aggregates of filamentous. circular and rod-shaped microstructures	limestones interbedded in diatomaceous and marly sediments.	Rouchy et al. (1998) Andreetto et al. (2019) Carpentier et al. (2020)
Caltanissetta Basin	southern part of Sicily (Italy)		The Miocene stratigraphic succession includes the: - **'Tripoli Formation**': diatomite formation with stromatolites beds at the top. - **'Calcare di Base'**: limestone beds separated by dolomite. calcareous marl. and rarely gypsum layers. - **'Calcare Solfifero**': diagenetic limestone with sulphur. - **'lower gypsum and salt units**': gypsum and salt. - **'Upper gypsum unit**': gypsum - **'Lago–Mare'**: brackish and freshwater facies.	Messinian	- sulphur-filled veins - powder-like native sulphur	– sulphur-rich coelestine - Sulphur bearing gypsum–carbonate - Porous and brecciated limestone - sulphur-bearing anhydrite	- Ziegenbalg et al. (2010) - Butler et al. (1995) - Oliveri et al. (2010)

by reaction of sulphuric acid with carbonates of the marls (Al-Juboury et al., 2006; Boudreau, 1991; Ziegenbalg et al., 2010). However, additional analyses, particularly isotope data are necessary to confirm their origin. It should be noted moreover that similar assemblages with natrojarosite, native sulphur, and gypsum have been described by Reolid et al. (2019) in the Lower Toarcian marls of the Cerradura section (SE Spain). The interpretation put forward involves BSR combined with anaerobic oxidation of methane cold seeps of methane produced in the sediments. The methane resulted from microbial methanogenesis of the organic-rich marls, moved within pore-space via diffusion or as bubbles that formed in the sediment patches (up to several decimetres in size) and subcylindrical concretions of yellowish powder. These features are reminiscent of those observed in the Tortonian and early Messinian marls of the Taza-Guercif basin interpreted as the result of anaerobic oxidation of biogenic methane by microbial activity (Figure 2; e.g. Felletti et al., 2020). Similar structures were also described in the Middle Miocene marls of the Fatha formation (Northern Iraq), associated with jarosite, alunite, silica-rich powder, and secondary gypsum (Al-Juboury et al., 2006) and ascribed to the reaction of marls with sulphuric acid generated by anaerobic oxidation and leaching of K, Na, Al, Fe and Ca. These structures were also interpreted in this case as an indication of sulphur occurrences reported in the area (Al-Juboury et al., 2006; Al-Sawaf, 1977). Finally, all markers in this area converge towards processes involving BSR activity, excluding TSR process because no thermal event was recorded in these 'post-nappes' basins developed by an extensive regime. It should also be noted that sulphuric acid could also be formed by sulphide oxidation when meteoric water percolates through lignite and cinerites present within Miocene Boudinar and Guercif basins. These conclusions remain to be confirmed by additional isotopes data.

6. Conclusion

The Neogene basins from the Moroccan Rif display similar stratigraphic successions and paleoenvironmental evolution to nearby Mediterranean basins including those of Southeastern Spain. Stratigraphic correlations show that the studied Moroccan Boudinar and Taza-Geurcif basins share with Spanish basins several stratigraphic and mineralogical characteristics. However, the numerous occurrences of native sulphur reported in the SE basins of Spain have not yet been firmly highlighted by any studies in northern Morocco. The current study shows the presence of favourable conditions for the formation of sulphur. Indeed, structures and mineralogical assemblies including jarosite, pyrite and gypsum generally associated with bacterially mediated sulphate reduction activity have been proposed in the Taza-Guercif area. Some are even associated with native sulphur, such as at the level of the nodules hosted in the marls of Oued-Amlil unit. Likewise, a structure generally associated with biogenic methane seeps have been identified at the level of the Guercif basin and are quite similar to existing structures in geological environments conducive to the native sulphur formation. In contrast, jarosite- and gypsum-bearing mineral assemblages more likely result from hydrothermal alteration related to the volcanic activity of the Ras Tarf volcano near the Boudinar basin. Despite this progress, further detailed field, petrological, and geochemical (mainly isotope data) studies of these Neogene formations are necessary to improve our understanding of the nature and origin of the sulphur-bearing formation.

Disclosure statement

No potential conflict of interest was reported by the author(s).

References

Achalhi, M., Münch, P., Cornée, -J.-J., Azdimousa, A., Melinte-Dobrinescu, M., Quillévéré, F., Drinia, H., Fauquette, S., Jiménez-Moreno, G., Merzeraud, G., Moussa, A. B., El Kharim, Y., & Feddi, N. (2016). The late miocene Mediterranean-Atlantic connections through the North Rifian Corridor: New insights from the Boudinar and Arbaa Taourirt basins (northeastern Rif, Morocco). *Palaeogeography, Palaeoclimatology, Palaeoecology*, *459* , 131–152. https://doi.org/10.1016/j.palaeo.2016.06.040

Al-Juboury, A. I., Al-Naqib, S. Q., & Al-Traif, A.-S. M. (2006). Mineralogical and geochemical study of the subsurface acidification products ninivite, alunite and jarosite, northern Iraq. *Arab Journal of Basic and Applied Sciences* 02 (01) 57–71 1815-3852 https://journal.uob.edu.bh/handle/123456789/426.

Al-Sawaf, F. D. S. (1977). Sulfate reduction and sulfur deposition in the lower fars formation, northern Iraq. *Economic Geology*, *72*(4), 608–618. https://doi.org/10.2113/gsecongeo.72.4.608

Amakrane, J., Azdimousa, A., Rezqi, H., El Hamouti, K., El Ouahabi, M., & Fagel, N. (2016). Paleoenvironment and sequence stratigraphy of the late miocene from the guercif basin (Northeastern of Morocco). *Bulletin de l'Institut Scientifique, Rabat* (38) , 95–110 2458-7184 http://www.israbat.ac.ma/wp-content/uploads/2017/07/Amakrane%20et%20al%2004%20Juillet%202017.pdf .

Anadón, P., Rosell, L., & Talbot, M. R. (1992). Carbonate replacement of lacustrine gypsum deposits in two Neogene continental basins, eastern Spain. *Sedimentary Geology*, *78*(3–4), 201–216. https://doi.org/10.1016/0037-0738(92)90020-R

Anadón, P., Ortí, F. and Rosell, L. (1997) Unidades evaporíticas de la zona de Libros-Cascante (Mioceno, Cuenca de Teruel): Características estratigraficas y sedimentológicas. Cuad. Geol. Iberica, 22, 283–304.

Andreetto, F., Dela Pierre, F., Gibert, L., Natalicchio, M., & Ferrando, S. (2019). Potential fossilized sulfide-oxidizing bacteria in the upper miocene sulfur-bearing limestones from the Lorca basin (SE Spain): Paleoenvironmental implications. *Frontiers in Microbiology*, *10 : 1031* . https://doi.org/10.3389/fmicb.2019.01031

Barré, G., Thomassot, É., Michels, R., Cartigny, P., Strzerzynski, P., & Truche, L. (2021). Multiple sulfur isotopes signature of thermochemical sulfate reduction (TSR): Insights from alpine triassic evaporites. *Earth and Planetary Science Letters*, *576* , 117231. https://doi.org/10.1016/j.epsl.2021.117231

Berner, R. A. (1970). Sedimentary pyrite formation. *American Journal of Science*, *268*(1), 1–23. https://doi.org/10.2475/ajs.268.1.1

Bernini, M., Boccaletti, M., Gelati, R., Moratti, G., Papani, G., & Mokhtari, J. E. (1999). Tectonics and sedimentation in the taza-guercif basin, Northern Morocco: Implications for the neogene evolution of the Rif-middle atlas orogenic system. *Journal of Petroleum Geology*, *22*(1), 115–128. https://doi.org/10.1111/j.1747-5457.1999.tb00462.x

Boudreau, B. P. (1991). Modelling the sulfide-oxygen reaction and associated pH gradients in porewaters. *Geochimica et Cosmochimica Acta*, *55*(1), 145–159. https://doi.org/10.1016/0016-7037(91)90407-V

Brahim, L. A., & Chotin, P. (1989). Genesis and deformation of the central Rif neogene basins (Morocco) during the closing up of European and African plates. *Geodinamica Acta*, *3* (4) , 295–304. https://doi.org/10.1080/09853111.1989.11105194

Butler, R. W., Lickorish, W. H., Grasso, M., Pedley, H. M., & Ramberti, L. (1995). Tectonics and sequence stratigraphy in Messinian basins, sicily: Constraints on the initiation and termination of the Mediterranean salinity crisis. *Geological Society of America Bulletin*, *107*(4), 425–439. https://doi.org/10.1130/0016-7606(1995)107<0425:TASSIM>2.3.CO;2

Butler, R. W. H., & Lickorish, W. H. (1997). Using high-resolution stratigraphy to date fold and thrust activity: Examples from the Neogene of south-central Sicily. *Journal of the Geological Society*, *154*(4), 633–643. https://doi.org/10.1144/gsjgs.154.4.0633

Calvo, J., Elizaga, E., Lopez-Martinez, N., Robles, F., & Usera, J. (1978). El Mioceno superior continental del Prebético externo: Evolución del estrecho nordbético. *Boletin Geologico y Minero*, *89*, 407–426 https://pascal-francis.inist.fr/vibad/index.php?action=getRecordDetail&idt=12720890.

Capella, W., Barhoun, N., Flecker, R., Hilgen, F. J., Kouwenhoven, T., Matenco, L. C., Sierro, F. J., Tulbure, M. A., Yousfi, M. Z., & Krijgsman, W. (2018). Palaeogeographic evolution of the late Miocene rifian corridor (Morocco): Reconstructions from surface and subsurface data. *Earth-Science Reviews*, *180* , 37–59. https://doi.org/10.1016/j.earscirev.2018.02.017

Carpentier, C., Vennin, E., Rouchy, J.-M., Cornée, -J.-J., Melinte-Dobrinescu, M., Hibsch, C., Olivier, N., Caruso, A., & Bartier, D. (2020). Ages and stratigraphical architecture of late Miocene deposits in the Lorca Basin (Betics, SE Spain): New insights for the salinity crisis in marginal basins. *Sedimentary Geology*, *405* , 105700. https://doi.org/10.1016/j.sedgeo.2020.105700

Caruso A, Pierre C, Blanc-Valleron M and Rouchy J. (2015). Carbonate deposition and diagenesis in evaporitic environments: The evaporative and sulphur-bearing limestones during the settlement of the Messinian Salinity Crisis in Sicily and Calabria. Palaeogeography, Palaeoclimatology, Palaeoecology, 429 136–162. 10.1016/j.palaeo.2015.03.035

Choubert, G., Charlot, R., Faure-Muret, A., Hottinger, L., Marcais, J., Tisserant, D., & Vidal, P. (1968). Note préliminaire sur le volcanisme messinien-(pontien) au Maroc. CR Acad. Sci. Paris, 266(série D), 197–199 http://pascal-francis.inist.fr/vibad/index.php?action=getRecordDetail&idt=GEODEBRGM6805004887 .

Choubert, G., Faure-Muret, A., Hilali, E. A., & Houzay, J. P., 1984. Carte géologique du Rif au 1/50.000, feuille Boudinar Notes et Mémoires du Service Géologique du Maroc N° 299 .

Colletta, B. (1977). Evolution néotectonique de la partie méridionale du bassin de Guercif (Maroc oriental) (Doctoral dissertation, Université Scientifique et Médicale de Grenoble).

Cornée, -J.-J., Münch, P., Achalhi, M., Merzeraud, G., Azdimousa, A., Quillévéré, F., Melinte-Dobrinescu, M., Chaix, C., Moussa, A. B., Lofi, J., Séranne, M., & Moissette, P. (2016). The Messinian erosional surface and early Pliocene reflooding in the Alboran Sea: New insights from the boudinar basin, Morocco. *Sedimentary Geology*, *333*, 115–129. https://doi.org/10.1016/j.sedgeo.2015.12.014

Decima, A., McKenzie, J. A., & Schreiber, B. C. (1988). The origin of" evaporitive" limestones; an example from the Messinian of Sicily (Italy). *Journal of Sedimentary Research*, *58*(2), 256–272. https://doi.org/10.1306/212F8D6E-2B24-11D7-8648000102C1865D

El Azzouzi, M., Bellon, H., Coutelle, A., & Réhault, J.-P. (2014). Miocene magmatism and tectonics within the Peri-Alboran orogen (western Mediterranean). *Journal of Geodynamics*, *77*, 171–185. https://doi.org/10.1016/j.jog.2014.02.006

El Desouky, H. A., Muchez, P., Boyce, A. J., Schneider, J., Cailteux, J. L., Dewaele, S., & von Quadt, A. (2010). Genesis of sediment-hosted stratiform copper–cobalt mineralization at Luiswishi and Kamoto, Katanga Copperbelt (democratic republic of Congo). *Mineralium Deposita*, *45*(8), 735–763. https://doi.org/10.1007/s00126-010-0298-3

El Kati, I., Benammi, M., Tabyaoui, H., & Benammi, M. (2017). Magnetostratigraphy of Neogene series of the Guercif basin (Morocco). *Rev. Soc. Geológica Esp*, *30* (2) , 37–50 2255-1379 https://sge.usal.es/archivos/REV/30(2)/RSGE30(2)_p_37_50.pdf .

Felletti, F., Marini, M., El Kati, I., & Tabyaoui, H. (2020). The Tachrift channel-levée turbidite complexes (Tortonian) of the Taza-Guercif basin (South Rifian Corridor, NE Morocco). *Journal of Maps*, *16*(2), 902–917. https://doi.org/10.1080/17445647.2020.1844088

García-Veigas, J., Rosell, L., Cendón, D. I., Gibert, L., Martín, J. M., Torres-Ruiz, J., & Ortí, F. (2015). Large celestine orebodies formed by early-diagenetic replacement of gypsified stromatolites (Upper Miocene, Montevive–Escúzar deposit, Granada Basin, Spain). *Ore Geology Reviews*, *64* (1) , 187–199. https://doi.org/10.1016/j.oregeorev.2014.07.009

Gelati R, Moratti G and Papani G. (2000). The Late Cenozoic sedimentary succession of the Taza-Guercif Basin, South Rifian Corridor, Morocco. Marine and Petroleum Geology, 17(3), 373–390. 10.1016/S0264-8172(99)00054-9

Iribarren, L., Vergés, J., & Fernàndez, M. (2009). Sediment supply from the Betic–Rif orogen to basins through Neogene. *Tectonophysics, the Geology of Vertical Movements of the Lithosphere*, *475* (1) , 68–84. https://doi.org/10.1016/j.tecto.2008.11.029

Jolivet, L., & Faccenna, C. (2000). Mediterranean extension and the Africa-Eurasia collision. *Tectonics*, *19*(6), 1095–1106. https://doi.org/10.1029/2000TC900018

Karikari-Yeboah, O., Skinner, W., & Addai-Mensah, J. (2019). Anaerobic pyrite oxidation in a naturally occurring pyrite-rich sediment under preload surcharge. *Environmental Monitoring and Assessment*, *191*(4), 1–11. https://doi.org/10.1007/s10661-019-7289-3

Krijgsman, W., Langereis, C. G., Zachariasse, W. J., Boccaletti, M., Moratti, G., Gelati, R., Iaccarino, S., Papani, G., & Villa, G. (1999). Late Neogene evolution of the Taza–Guercif Basin (Rifian Corridor, Morocco) and implications for the Messinian salinity crisis. *Marine Geology*, *153*(1–4), 147–160. https://doi.org/10.1016/S0025-3227(98)00084-X

Kutney, G. (2007). *Sulfur: History, technology, applications & industry*. ChemTec Publishing.

Labrado, A. L., Brunner, B., Bernasconi, S. M., & Peckmann, J. (2019). Formation of large native sulfur deposits does not require molecular oxygen. *Frontiers in Microbiology*, *10*. https://doi.org/10.3389/fmicb.2019.00024

Lindtke, J., Ziegenbalg, S. B., Brunner, B., Rouchy, J. M., Pierre, C., & Peckmann, J. (2011). Authigenesis of native sulphur and dolomite in a lacustrine evaporitic setting (Hellín basin, Late Miocene, SE Spain). *Geological Magazine*, *148*(4), 655–669. https://doi.org/10.1017/S0016756811000124

Lueth, V. W., Rye, R. O., & Peters, L. (2005). "Sour gas" hydrothermal jarosite: Ancient to modern acid-sulfate mineralization in the southern Rio Grande Rift. Chem. Geol., Geochemistry of Sulfate Minerals: A tribute to Robert O. *Rye*, *215* (1–4) , 339–360. https://doi.org/10.1016/j.chemgeo.2004.06.042

Machel, H. G. (2001). Bacterial and thermochemical sulfate reduction in diagenetic settings — Old and new insights. *Sedimentary Geology*, *140*(1–2), 143–175. https://doi.org/10.1016/S0037-0738(00)00176-7

Martinez-Frias, J., Amaral, G., & Vázquez, L. (2006). Astrobiological significance of minerals on Mars surface environment. *Reviews in Environmental Science and Bio/Technology*, *5*(2–3), 219–231. https://doi.org/10.1007/s11157-006-0008-x

Merzeraud, G., Achalhi, M., Cornée, -J.-J., Münch, P., Azdimousa, A., & Ben Moussa, A. (2019). Sedimentology and sequence stratigraphy of the late-Messinian - Early pliocene continental to marine deposits of the Boudinar basin (North Morocco). *Journal of African Earth Sciences*, *150*, 205–223. https://doi.org/10.1016/j.jafrearsci.2018.11.002

Muchez, P., André-Mayer, A. S., El Desouky, H. A., & Reisberg, L. (2015). Diagenetic origin of the stratiform Cu–Co deposit at kamoto in the central African copperbelt. *Mineralium Deposita*, *50*(4), 437–447. https://doi.org/10.1007/s00126-015-0582–3

Newhall, C. G., & Dzurisin, D. (1988). *Historical unrest at the large calderas of the world*. Department of the Interior, US Geological Survey.

Oliveri, E., Neri, R., Bellanca, A., & Riding, R. (2010). Carbonate stromatolites from a Messinian hypersaline setting in the caltanissetta basin, sicily: Petrographic evidence of microbial activity and related stable isotope and rare earth element signatures. *Sedimentology*, *57*(1), 142–161. https://doi.org/10.1111/j.1365-3091.2009.01094.x

Orti F, Rosell L and AnadON P. (2003). Deep to shallow lacustrine evaporites in the Libros Gypsum (southern Teruel Basin, Miocene, NE Spain): an occurrence of pelletal gypsum rhythmites. Sedimentology, 50(2), 361–386. 10.1046/j.1365-3091.2003.00558.x

Ortí, F., Rosell, L., & Anadón, P. (2010). Diagenetic gypsum related to sulfur deposits in evaporites (Libros Gypsum, Miocene, NE Spain). *Sedimentary Geology*, *228*(3–4), 304–318. https://doi.org/10.1016/j.sedgeo.2010.05.005

Pérez-Asensio, J. N., Aguirre, J., Jiménez-Moreno, G., Schmiedl, G., & Civis, J. (2013). Glacioeustatic control on the origin and cessation of the Messinian salinity crisis. *Global and Planetary Change*, *111*, 1–8. https://doi.org/10.1016/j.gloplacha.2013.08.008

Pineda, V., Gibert, L., Soria, J. M., Carrazana, A., Ibáñez-Insa, J., & Sánchez-Román, M. (2021). Interevaporitic deposits of Las Minas Gypsum Unit: A record of Late Tortonian marine incursions and dolomite precipitation in Las Minas Basin (eastern Betic Cordillera, SE Spain). *Palaeogeography, Palaeoclimatology, Palaeoecology*, *564*, 110171. https://doi.org/10.1016/j.palaeo.2020.110171

Platt, J. P., Behr, W. M., Johanesen, K., & Williams, J. R. (2013). The betic-Rif Arc and its orogenic hinterland: A review. *Annual Review of Earth and Planetary Sciences*, *41*(1), 313–357. https://doi.org/10.1146/annurev-earth-050212-123951

Pratt, J. R., Barbeau, D. L., Izykowski, T. M., Garver, J. I., & Emran, A. (2016). Sedimentary provenance of the Taza-Guercif Basin, South Rifean Corridor, Morocco: Implications for basin emergence. *Geosphere*, *12*(1), 221–236. https://doi.org/10.1130/GES01192.1

Reolid, M., Abad, I., & Benito, M. I. (2019). Upper Pliensbachian-Lower Toarcian methane cold seeps interpreted from geochemical and mineralogical characteristics of celestine concretions (South Iberian palaeo-margin). *Palaeogeography, Palaeoclimatology, Palaeoecology*, *530*, 15–31. https://doi.org/10.1016/j.palaeo.2019.05.033

Rodríguez, A., & van Bergen, M. J. (2015). Volcanic hydrothermal systems as potential analogues of Martian sulphate-rich terrains. *Netherlands Journal of Geosciences*, *95* (2) , 153–169. https://doi.org/10.1017/njg.2015.12

Rodríguez, A., & van Bergen, M. J. (2017). Superficial alteration mineralogy in active volcanic systems: An example of Poás volcano, Costa Rica. *Journal of Volcanology and Geothermal Research* VolcanoHydrothermal Systems, VolcanoHydrothermal Systems, *346*, 54–80. https://doi.org/10.1016/j.jvolgeores.2017.04.006

Rossi F Paolo, Schito A, Manzi V, Roveri M, Corrado S, Lugli S and Reghizzi M. (2021). Paleo-thermal constraints on the origin of native diagenetic sulfur in the Messinian evaporites: The Northern Apennines foreland basin case study (Italy). Basin Res, 33(4), 2500–2516. 10.1111/bre.12566

Rouchy, J. M., Taberner, C., Blanc-Valleron, -M.-M., Sprovieri, R., Russell, M., Pierre, C., Di Stefano, E., Pueyo, J. J., Caruso, A., Dinarès-Turell, J., Gomis-Coll, E., Wolff, G. A., Cespuglio, G., Ditchfield, P., Pestrea, S., Combourieu-Nebout, N., Santisteban, C., & Grimalt, J. O. (1998). Sedimentary and diagenetic markers of the restriction in a marine basin: The Lorca Basin (SE Spain) during the Messinian. *Sedimentary Geology*, *121*(1–2), 23–55. https://doi.org/10.1016/S0037-0738(98)00071-2

Roveri, M., Flecker, R., Krijgsman, W., Lofi, J., Lugli, S., Manzi, V., Sierro, F. J., Bertini, A., Camerlenghi, A., De Lange, G., Govers, R., Hilgen, F. J., Hübscher, C., Meijer, P. T., & Stoica, M. (2014). The Messinian salinity crisis: Past and future of a great challenge for marine sciences. *Mar. Geol*, *352*, 25–58. 50th Anniversary Special Issue. https://doi.org/10.1016/j.margeo.2014.02.002

Ruckmick, J. C., Wimberly, B. H., & Edwards, A. F. (1979). Classification and genesis of biogenic sulfur deposits. *Economic Geology*, *74*(2), 469–474. https://doi.org/10.2113/gsecongeo.74.2.469

Sælen, G., Lunde, I. L., Walderhaug Porten, K., Braga, J. C., Dundas, S. H., Ninnemann, U. S., Ronen, Y., & Talbot, M. R. (2016). Oyster shells as recorders of short-term oscillations of salinity and temperature during deposition of coral bioherms and reefs in the Miocene Lorca basin, SE Spain. *Journal of Sedimentary Research*, *86*(6), 637–667. https://doi.org/10.2110/jsr.2016.18

Sani, F., Zizi, M., & Bally, A. W. (2000). The Neogene–quaternary evolution of the Guercif Basin (Morocco) reconstructed from seismic line interpretation. *Marine and Petroleum Geology*, *17*(3), 343–357. https://doi.org/10.1016/S0264-8172(99)00058-6

Scher, S., Williams-Jones, A. E., & Williams-Jones, G. (2013). Fumarolic activity, acid-sulfate alteration, and high sulfidation epithermal precious metal mineralization in the crater of kawah ijen volcano, java, Indonesia. *Economic Geology*, *108* (5), 1099–1118. https://doi.org/10.2113/econgeo.108.5.1099

Serafimovski, T., Tasev, G., & Gjorgiev, L., 2015. Sulfur isotope composition in the plesenci native sulfur mineral deposit, republic of Macedonia. *Procedia Earth Planet. Sci., 11th Applied Isotope Geochemistery Conference AIG-11* 13, 35–38. https://doi.org/10.1016/j.proeps.2015.07.008

Servant-Vildary, S. (1986). Fossil CycZoteZZa Species from Miocene LacustrineDeposit of Spain.

Servant-Vildary, S., Rouchy, J. M., Pierre, C., & Foucault, A. (1990). Marine and continental water contributions to a hypersaline basin using diatom ecology, sedimentology and stable isotopes: An example in the Late Miocene of the Mediterranean (Hellin Basin, southern Spain). *Palaeogeography, Palaeoclimatology, Palaeoecology*, *79*(3–4), 189–204. https://doi.org/10.1016/0031-0182(90)90017-2

Suter, G. 1980. *Carte géologique de la chaine rifaine au 1/500 000*. Notes et Mémoire du service géologique du Maroc N° 245a.

Vaitkus A, Merkys A and Gražulis S. (2021). Validation of the Crystallography Open Database using the Crystallographic Information Framework. J Appl CrystallogrJ Appl Cryst, 54 (2), 661–672. 10.1107/S1600576720016532/yr5065sup1.pdf

Vithana, C. L., Sullivan, L. A., Burton, E. D., & Bush, R. T. (2015). Stability of schwertmannite and jarosite in an acidic landscape: Prolonged field incubation. *Geoderma*, *239*, 47–57. https://doi.org/10.1016/j.geoderma.2014.09.022

Wagenfeld, J.-G., Al-Ali, K., Almheiri, S., Slavens, A. F., & Calvet, N. (2019). Sustainable applications utilizing sulfur, a by-product from oil and gas industry: A state-of-the-art review. *Waste Management*, *95*, 78–89. https://doi.org/10.1016/j.wasman.2019.06.002

Whitworth, A. J., Brand, H. E. A., Wilson, S. A., & Frierdich, A. J. (2020). Iron isotope geochemistry and mineralogy of jarosite in sulfur-rich sediments. *Geochimica et Cosmochimica Acta*, *270*, 282–295. https://doi.org/10.1016/j.gca.2019.11.029

Ziegenbalg, S. B., Brunner, B., Rouchy, J. M., Birgel, D., Pierre, C., Böttcher, M. E., Caruso, A., Immenhauser, A., & Peckmann, J. (2010). Formation of secondary carbonates and native sulphur in sulphate-rich Messinian strata, Sicily. *Sedimentary Geology*, *227*(1–4), 37–50. https://doi.org/10.1016/j.sedgeo.2010.03.007

Znamenskiy, V. S. (1990). zoning of alteration around solfataras of the kurile volcanoes. *International Geology Review*, *32*(7), 683–691. https://doi.org/10.1080/00206819009465810